Al-Khwarizmi Engineering Journal, Vol. 4, No. 4, PP 45-56 (2008)

Al-Khwarizmi Engineering Journal

Parametric Study of Mixed Convective Radiative Heat Transfer in an Inclined Annulus

Manal H. Al-Hafidh **Raed G. Saihood**

Departement of Mechanical Engineering/ University of Baghdad

(Received 11 September 2007; accepted 11 September 2008)

Abstract

The steady state laminar mixed convection and radiation through inclined rectangular duct with an interior circular tube is investigated numerically for a thermally and hydrodynamicaly fully developed flow. The two heat transfer mechanisms of convection and radiation are treated independently and simultaneously. The governing equations which used are continuity, momentum and energy equations. These equations are normalized and solved using the Vorticity-Stream function and the Body Fitted Coordinates (B.F.C) methods. The finite difference approach with the Line Successive Over-Relaxation (LSOR) method is used to obtain all the computational results. The (B.F.C) method is used to generate the grid of the problem. A computer program (Fortran 90) is built to calculate the steady state Nusselt number (Nu) for Aspect Ratio AR (0.55-1) and Geometry Ratio GR (0.1-0.9). The fluid Prandtl number is 0.7, Rayleigh number Ra = 400, Reynolds number Re = 100, Optical Thickness ($0 \leq t \leq 10$), Conduction- Radiation parameter ($0 \leq N \leq 100$) and Inclination angle $\lambda = 45$. For the range of parameters considered, results show that radiation enhance heat transfer. It is also indicated in the results that heat transfer from the surface of the circle exceeds that of the rectangular duct. Generally, Nu is increased with increasing GR, t and N but it decreased with AR increase. When the radiation effect added to the heat transfer mechanism, the heat transfer rate increased. This effect increased with increasing in GR and decreasing with AR. The increasing in radiation properties lead to increase the radiation effect. Tecplot 7 program was used to plot the curves which cleared these relations and isotherms and streamlines which illustrate the behavior of air through the channel and its variation with other parameters. A correlation equation is concluded to describe the radiation effect. Comparison of the results with the previous work shows a good agreement.

Keywords: Mixed Convection, Radiation, Rectangular Duct, Circular Tube, Laminar Flow.

1. Introduction:

Various heat transfer mechanisms and geometries have been studied by some engineers and scientists purposely to augment heat transfer in heat exchangers and some other heat transfer equipments. A numerical study of natural convection in horizontal elliptic cylinder was studied by (Bello-Ochende, 1985) and (Siegel, 1985) also analyzed the effect of buoyancy on heat transfer in a rotating tube. A perturbation analysis of combined free and forced laminar convection in a tilted elliptic cylinder was carried out by (Bello-Ochende and Adegun, 1993). Thermal radiation and laminar forced convection in the entrance region of a pipe with axial conduction and radiation were considered by (Yang and Ebadian, 1991) and (Dong et al, 1993) employed the geometry combination of a square duct with a centered circular core for the design of an oven for heat treatment of ceramic and metallic products. They studied a situation where the central core is solid. Combined natural convection- conduction and radiation heat transfer in discretely open cavity was studied by (Dehgham et al, 1996) and (Bello-Ochende and Adegun, 2002) also worked on combined convective and radiative heat transfer in a tilted, rotating, uniformly heated square duct with a centered circular cylinder. The work under investigation is to augment heat transfer in heat exchangers using geometric combination of a rectangular duct and a circular core. The working fluid flows between the inner surface of the rectangular duct and outer surface of the circular cylinder.

2. Mathematical Model:

The schematic drawing of the geometry and the Cartesian coordinate system employed in solving the problem is shown in Fig.(1).

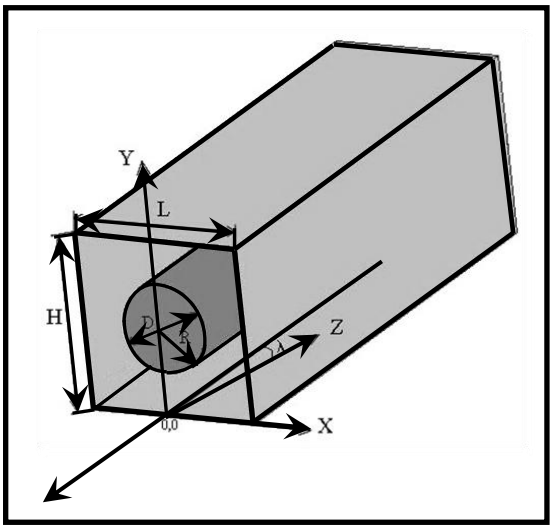

Fig. 1. Schematic of The Problem Geometry.

The fluid flows between the circular tube and the rectangular duct (Annulus). This annulus is symmetrical about Y-axis ($\partial/\partial x = 0$). The width and height of the channel are L and H respectively. The diameter and radius of tube are D and R respectively and the hydraulic diameter is d:

$$d = \frac{4A}{p^*} = \frac{2(HL - \pi R^2)}{(H + L + \pi R)} \qquad ...(1)$$

The flow is upward, steady state, hydrodynamically and thermally fully developed laminar flow. Symmetrical three-dimensional flow (symmetry about y-axis). The working fluid is assumed absorbing and emitting. Heat transfer mechanism is convection (free-forced) and radiation. Viscous dissipation affect in energy equation is negligible. Boussineq approximation is used which means that the fluid density is assumed constant except when it directly causes buoyant forces (in momentum equation). All other fluid properties are assumed constant (Newtonian fluid). The axial (z-direction) shown in Fig.(1) is the predominant direction for the fluid flow. A viscous dissipation effect is neglected. Axial conduction and radiation are assumed negligible following (Yang and Ebadian, 1991) for a condition that (Re Pr t / H) >10.

Governing Equations:

The governing equations are:

Continuity Equation:

$$\frac{\partial u}{\partial x} + \frac{\partial v}{\partial y} = 0 \qquad ...(2)$$

Momentum Transport Equation:

The momentum transport equations in the x, y and z directions are respectively:

$$u\frac{\partial u}{\partial x} + v\frac{\partial x}{\partial y} = -\frac{1}{\rho}\frac{\partial p}{\partial x} + \nu\nabla^2 u \qquad ...(3)$$

$$u\frac{\partial u}{\partial x} + v\frac{\partial v}{\partial y} =$$

$$-\frac{1}{\rho}\frac{\partial p}{\partial y} + \nu\nabla^2 u - \beta g(T_w - T)\cos\lambda \qquad ...(4)$$

$$u\frac{\partial w}{\partial x} + v\frac{\partial w}{\partial y} =$$

$$-\frac{1}{\rho}\frac{\partial p}{\partial z} + \nu\nabla^2 w - \beta g(T_w - T)\sin\lambda \qquad ...(5)$$

Energy Transport Equation:

In the absence of energy sources and viscous energy dissipation, the energy equation for steady flow, with radiation incorporated is:

$$u\frac{\partial T}{\partial x} + v\frac{\partial T}{\partial y} + w\frac{\partial T}{\partial z} = \alpha\left(\frac{\partial^2 y}{\partial x^2} + \frac{\partial^2 y}{\partial x^2}\right)$$

$$+\frac{\sigma K_R \varepsilon}{\rho c_p}\left(T_w^4 - T^4\right) \qquad ...(6)$$

The boundary conditions for these equations are:

$$T = T_w$$
$$U = V = W = 0$$

Vorticity-Stream Function Method:

This method is used to eliminate the pressure terms in the two momentum equations in x and y directions by cross differentiation to the equations (3) and (4):

$$\frac{\partial u}{\partial x}\frac{\partial u}{\partial x}+u\frac{\partial^2 u}{\partial x\partial y}+\frac{\partial v}{\partial y}\frac{\partial u}{\partial y}+v\frac{\partial^2 u}{\partial y^2}=-\frac{\partial^2 p}{\partial x\partial y}$$

$$+\left(\frac{\partial^3 u}{\partial y^2\partial y}+\frac{\partial^3 y}{\partial y^3}\right) \qquad ...(7)$$

$$\frac{\partial u}{\partial x}\frac{\partial v}{\partial x}+u\frac{\partial^2 v}{\partial x^2}+\frac{\partial v}{\partial y}\frac{\partial v}{\partial y}+v\frac{\partial^2 v}{\partial y\partial x}=-\frac{\partial^2 p}{\partial x\partial y}$$

$$+\left(\frac{\partial^3 v}{\partial x^3}+\frac{\partial^3 u}{\partial y^2\partial x}\right)+\frac{Ra\cos\lambda}{\mathrm{Pr}}\frac{\partial\theta}{\partial x} \qquad ...(8)$$

By subtracting equation (7) from (8) and substitute vorticity definition, the following equation can be obtained:

$$u\frac{\partial w}{\partial x}+v\frac{\partial w}{\partial y}=\frac{\partial^2 w}{\partial x^2}+\frac{\partial^2 w}{\partial y^2}-\frac{Ra\cos\lambda}{\mathrm{Pr}}\frac{\partial\theta}{\partial x} \quad ...(9)$$

Normalization Parameters:

The variables in the governing equations and boundary conditions are transformed to dimensionless formula by employing the following transformation parameters:

$$\mathrm{X}=\frac{x}{d}\ ,\quad Y=\frac{y}{d}\ ,\quad Z=\frac{z}{d}$$

$$U=\frac{ud}{v}\ ,\quad V=\frac{vd}{v}\ ,\quad W=\frac{wd}{v}$$

$$\theta=\frac{T}{T_w}\ ,\ \frac{\partial p}{\partial z}=-\frac{4\rho v^2}{d^3}\mathrm{Re}\ ,\ \frac{\partial T}{\partial z}=\frac{T_w}{\mathrm{Pr}\,d}\ ,\ \mathrm{Pr}=\frac{v}{a}$$

$$N=\frac{4\sigma\varepsilon T_w^3}{K_R k}\ ,\ t=K_R d\ ,\ U=\frac{\partial\psi}{\partial Y}\ ,\ V=-\frac{\partial\psi}{\partial X}$$

By using the relation above the equations (5, 6 and 9) became:

Vorticity Definition Equation:

$$-\omega=\frac{\partial^2\psi}{\partial X^2}+\frac{\partial^2\psi}{\partial Y^2} \qquad ...(10)$$

Momentum Equations:

$$\frac{\partial\psi}{\partial Y}\frac{\partial\omega}{\partial X}-\frac{\partial\psi}{\partial X}\frac{\partial\omega}{\partial Y}=\left(\frac{\partial^2\omega}{\partial x^2}+\frac{\partial^2\omega}{\partial Y^2}\right)$$

$$-\frac{Ra\cos\lambda}{\mathrm{Pr}}\frac{\partial\theta}{\partial X} \qquad ...(11)$$

$$\frac{\partial\psi}{\partial Y}\frac{\partial W}{\partial X}-\frac{\partial\psi}{\partial X}\frac{\partial W}{\partial Y}=\left(\frac{\partial^2 W}{\partial X^2}+\frac{\partial^2 W}{\partial Y^2}\right)$$

$$+4\,\mathrm{Re}-\frac{Ra\sin\lambda}{\mathrm{Pr}}(1-\theta) \qquad ...(12)$$

Energy Equation:

$$\frac{\partial\psi}{\partial Y}\frac{\partial\theta}{\partial X}-\frac{\partial\psi}{\partial X}\frac{\partial\theta}{\partial Y}=\frac{1}{\mathrm{Pr}}\left(\frac{\partial^2\theta}{\partial X^2}+\frac{\partial^2\theta}{\partial Y^2}\right)$$

$$-\frac{W}{\mathrm{Pr}}+\frac{Nt^2}{4\,\mathrm{Pr}}(1-\theta^4) \qquad ...(13)$$

The boundary conditions applicable to these equations are (Fig. 2):

(1) At the inlet of the duct (Z = 0):

$$U=V=\psi=\omega=0$$
$$\theta=0.5,\quad W=\mathrm{Re}$$

(2) At the walls:

$$U=V=W=\psi=0$$
$$\theta=1$$

$$\frac{\partial\theta}{\partial X}=\frac{\partial\psi}{\partial X}=\frac{\partial\omega}{\partial \mathrm{X}}=\frac{\partial W}{\partial \mathrm{X}}=0\ (symmetry\ plane)$$

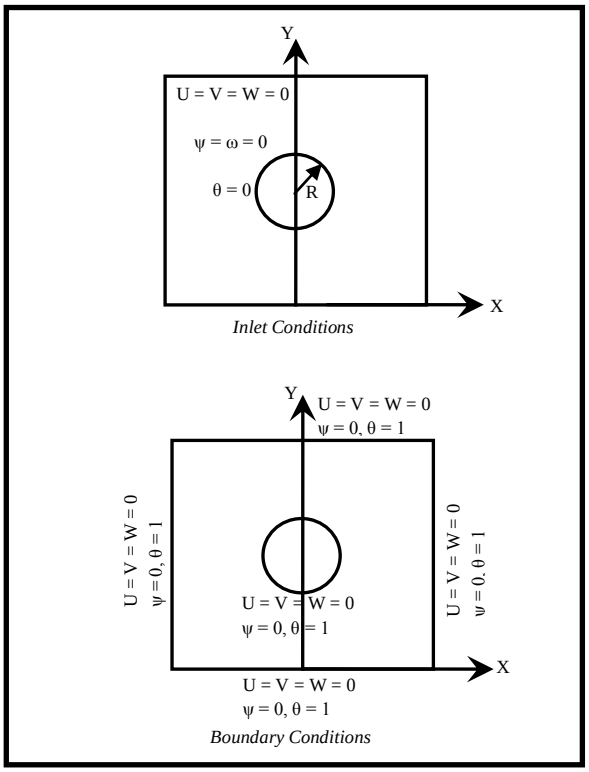

Fig. 2. The Inlet and Boundary Conditions.

3. Numerical Solution:

Numerical Grid Generation:

The elliptic transformation technique which was originally proposed by (Fletcher, 1988) is applied to generate the curvilinear grid for dealing with the irregular cross sections. The transformation functions $\xi = \xi(X,Y)$ and $\eta = \eta(X,Y)$ are obtained to accommodate the irregular shape by solving the following partial differential equations:

$$\frac{\partial^2 \xi}{\partial X^2} + \frac{\partial^2 \xi}{\partial Y^2} = G(\xi,\eta) \qquad ...(14.a)$$

$$\frac{\partial^2 \eta}{\partial X^2} + \frac{\partial^2 \eta}{\partial Y^2} = S(\xi,\eta) \qquad ...(14.b)$$

where G and S are two functions which are defined to artificially adjust the density of the grid locally. Using the curvilinear grid obtained, the governing eq. (10-13) and the boundary conditions are then discretized and solved in the computation domain (ξ,η).

In this work, an (81 X 61) grid in the transformed domain $(\xi \times \eta)$ is adopted. Fig.(3) shows typical grid generated for the channel cross section. The grid systems have been properly adjusted to be orthogonal locally at the boundaries.

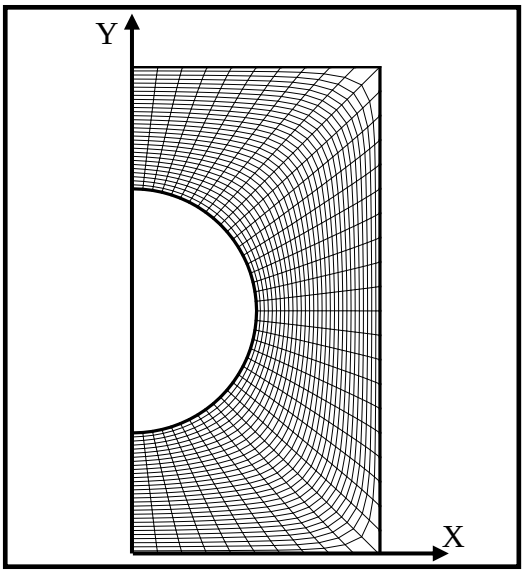

Fig. 3. The Generated Grid.

By using this method, the following general equation can be used to generate all the governing equations (10-13) in computational coordinates formula:

$$J\Gamma\left(\psi_\eta \phi_\xi - \psi_\xi \phi_\eta\right) = \left(\tau\phi_\xi + \varpi\phi_\eta + \alpha_1\phi_{\xi\xi} - 2\beta_1\phi_{\xi\eta} + \gamma\phi_{\eta\eta}\right) + suJ^2 \qquad ...(15)$$

Where ϕ represent the general variable which may be ω, W or θ and su is the source term.

4. Finite Difference Formulation:

The three-point central difference formula is applied to all the derivatives. Each of the governing equations can be rewritten in a general form as:

$$ap_{(i.j)}\phi_{(i,j)} = ae_{(i,j)}\phi_{(i+1,j)} + aw_{(i,j)}\phi_{(i-1,j)} + an_{(i,j)}\phi_{(i,j+1)} + as_{(i,j)}\phi_{(i,j-1)} + SU_{(i,j)}J_{(i,j)} \qquad ...(16)$$

where:

$$ap_{(i,j)} = 2\left(\alpha_{1(i,j)} + \gamma_{(i,j)}\right)$$

$$ae_{(i,j)} = \alpha_{1(i,j)} - B$$

$$aw_{(i,j)} = \alpha_{1(i,j)} + B$$

$$an_{(i,j)} = \gamma_{(i,j)} - C$$

$$as_{(i,j)} = \gamma_{(i,j)} + C$$

$$B = \left(J_{(i,j)}\Gamma \frac{\psi_{(i+1,j)} - \psi_{(i-1,j)}}{2} - \tau_{(i,j)} \right) \Big/ 2$$

$$C = \left(- J_{(i,j)}\Gamma \frac{\psi_{(i,j+1)} - \psi_{(i,j-1)}}{2} - \varpi_{(i,j)} \right) \Big/ 2$$

$$SU_{(i,j)} = -\frac{\beta_{1(i,j)}}{2J_{(i,j)}}\left(\phi_{(i+1,j-1)} - \phi_{(i-1,j+1)} - \phi_{(i-1,j+1)} + \phi_{(i-1,j-1)} + su_{(i,j)}J_{(i,j)}\right)$$

In the equations above i and j indicate to the points of the grid in the generalized coordinates ξ and η respectively.

As pointed out in (Anderson, 1984) the Relaxation method can be employed for the numerical solution of the eq. (10). For this study, the LSOR method [Fletcher, 1988 and Anderson, 1984] is used to solve equations (11, 12 and 13). The convergence criterion for the inner iteration ($Error_{in}$) of ψ is 10^{-4} and for the outer iteration ($Error_{out}$) of θ_b is 10^{-10}, where:

$$Error_{in} = 2\left(\alpha_{1(i,j)} + \gamma_{(i,j)}\right)\Delta\psi_{(i,j)} \qquad ...(17)$$

$$\Delta\psi_{(i,j)} = \frac{\psi_{(i,j)}^{it+1} - \psi_{(i,j)}^{it}}{RP} \qquad ...(18)$$

where RP is the Relaxation Parameter and equal to 1.1 and it represent the number of iterations. The outer iteration is checked only for θ_b as follow:

$$Error_{out} = \frac{\theta_b^{it+1} - \theta_b^{it}}{\theta_b^{it}} \le 10^{-10} \qquad ...(19)$$

5. Evaluation of Heat Transfer:

The peripheral heat transfer is defined through the conduction referenced Nusselt number as:

Local Nusselt number:

The peripheral local Nusselt number on the walls of the channel is computed from [Bello-Ochende & Adegun]:

$$Nu_L = \frac{-\left.\frac{\partial\theta}{\partial n}\right|_w}{1-\theta_b} \qquad ...(20)$$

where n represent the normal outward unit vector.

The mean Nusselt number on the wall of the rectangular duct and circular tube is obtained by using Simpson's rule:

$$Nu_{c,r} = \frac{1}{s}\int_S Nu_L\, ds \qquad ...(21)$$

where s represents the length of the wetted perimeter in the rectangular duct and circular tube.

The mean Nusselt number (Nu) is a measure of the average heat transfer over the internal surface of the rectangular duct and the outer surface of the circular configuration. It is computed from the following equation [Bello-Ochende & Adegun]:

$$Nu = C_C Nu_C + C_r Nu_r \qquad ...(22)$$

where, C_C Nu_C is a measure of average heat transfer from the outer surface of the circular core while C_r Nu_r corresponds to heat transfer from of the internal surface of the rectangular duct. C_c and C_r are the perimetric ratios for the heat transfer and are defined as:

$$C_c = \frac{\pi R}{H + L + \pi R}$$

$$C_r = \frac{H + L}{H + L + \pi R}$$

6. Results and Discussion:

Results are presented for the following ranges of parameters:

$0.1 \le GR \le 0.9$
$0.55 \le AR \le 1$
$0 \le N \le 100$
$0 \le t \le 10$
Re = 100, Ra = 400, Pr = 0.7

6.1 Comparison of Results:

The comparison was made for the value of Nu_L at the walls of the channel (rectangular duct and circular tube) with the previous results obtained by Bello-Ochende & Adegun. These comparisons are shown in Figs. (4a) and (4b). From these figures, a difference (approximately 10%) is found between these results.

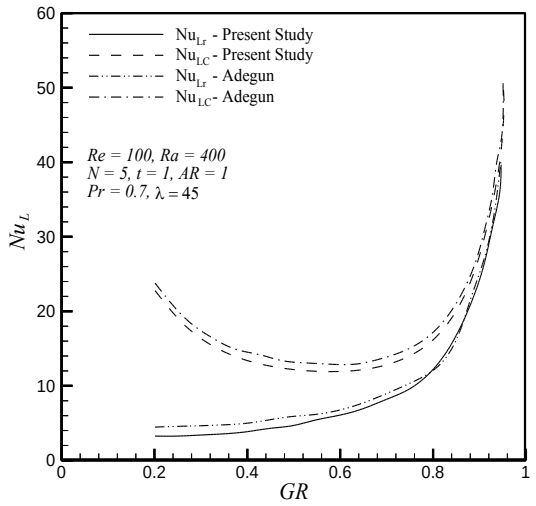

Fig.4a. Comparison Results (without radiation).

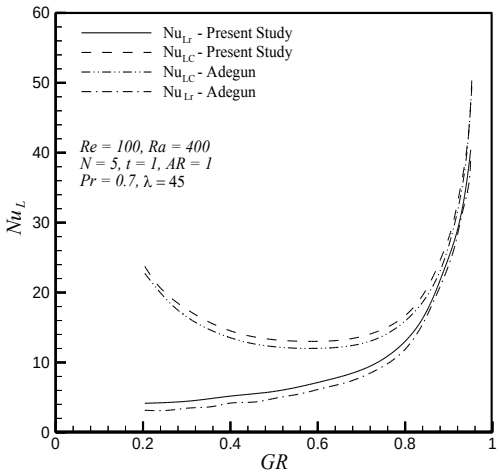

Fig.4b. Continued (with Radiation).

The number of nodes in ξ and η directions has very small effect on the value of Nusselt number on the walls of the channel as shown in Figs (5a) and (5b).

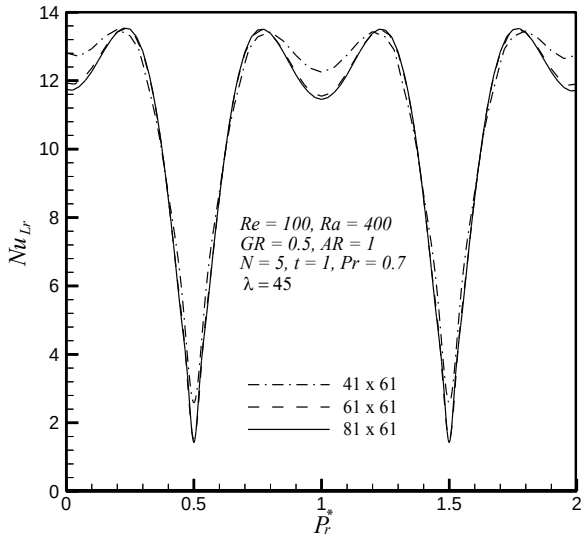

Fig.5a. The Variation Of Nu_{lr} On The Rectangular Duct Walls With The Number of Nodes (along ξ).

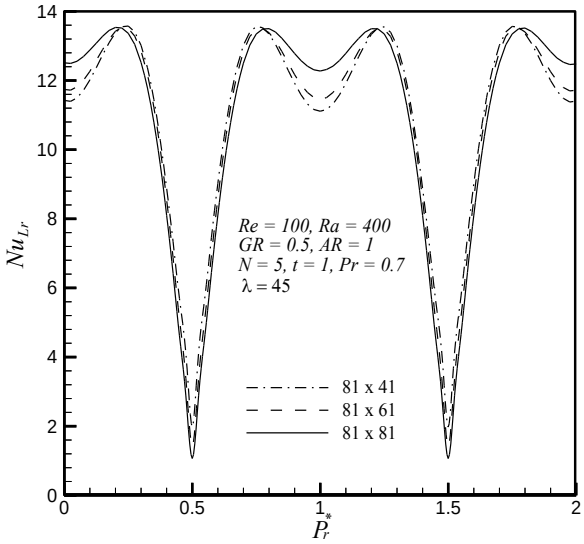

Fig.5b. Continued (along η).

6.2 Effect of GR:

The heat transfer process through the channel suffers from many changes due to the layer of the still air in the corners as shown in Figs (6-8). This layer cause to increase the thermal resistance and that lead to decrease the rate of heat transfer. The heat transfer rate through the wall of the circular tube is uniform and greater than that on the walls of the rectangular duct. The direction of the heat transfer from the walls towards the core of the

channel is shown by the isotherm lines. When GR is larger than 0.2, two cells will be generated and the center of these cells had a minimum temperature. As shown in Figs (6-8), the volume of these cells decreased with increasing GR value and that because of the decreasing of the confined area between the walls and the temperature of these cells increased.

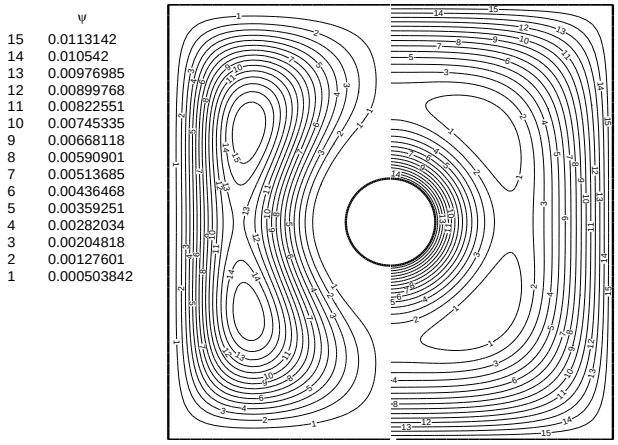

Fig.6. Streamlines and Isotherms for GR = 0.4.

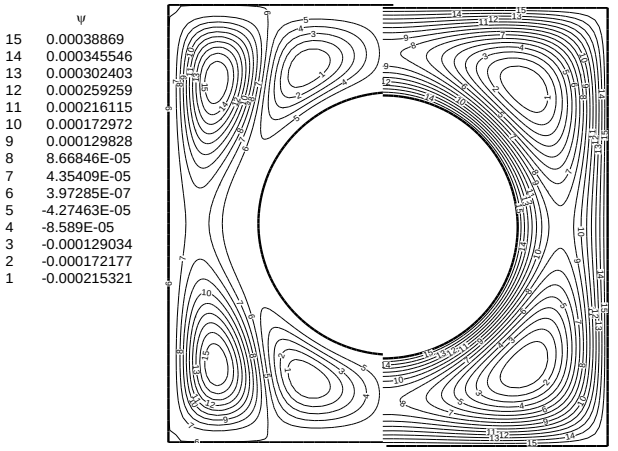

Fig.7. Streamlines and Isotherms for GR = 0.6.

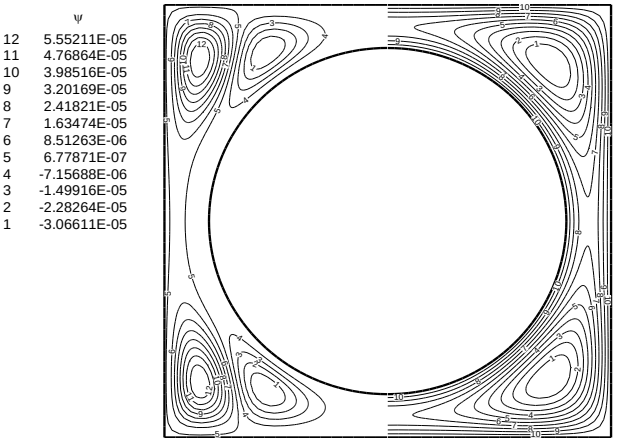

Fig.8. Streamlines and Isotherms for GR = 0.8.

Streamlines are shown in Figs. (6-8). With increasing the value of GR, two cells will be generated inside this big cell. The maximum value of stream function is at the center of these two cells. When GR increased greater than 0.2, two additional cells will be generated and their centers have the minimum value of the stream function. These cells are generated because of the difference between the velocity of particles in the hot and cold regions, in addition to the impact between the rising and lowering air streams. The volume of these cells will be decreased with increasing in GR value until small four cells generated.

Fig. (9) illustrates the variation of mean Nusselt number Nu through the channel with GR value. It is shown that when GR increased then Nu increased, this is due to the effect of increasing in the surface area of the circular wall. This increasing of the surface area leads to increase the rate of heat transfer. The radiation effect is very small for the small values of GR. This effect increased with increasing in GR value because of increasing the heat gain by air with decreasing in the air quantity.

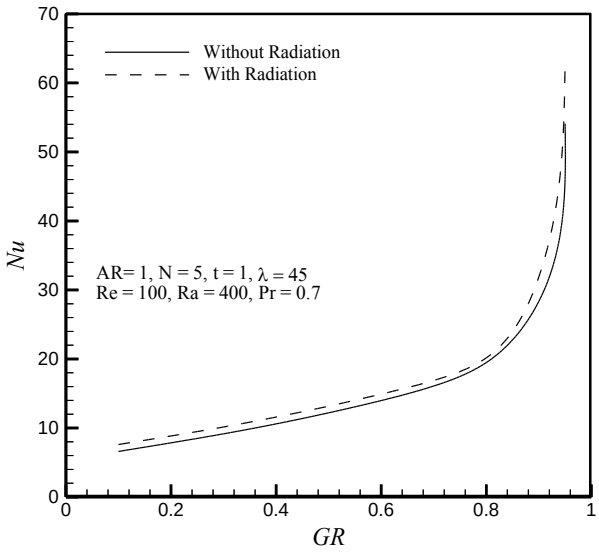

Fig. 9. The Variation of Nu With GR

The bulk temperature of air increased with increasing in GR value as shown in Fig. (10) and that because of increasing in the surface area which participating in the heat transfer process and that result to increase the rate of heat transfer.

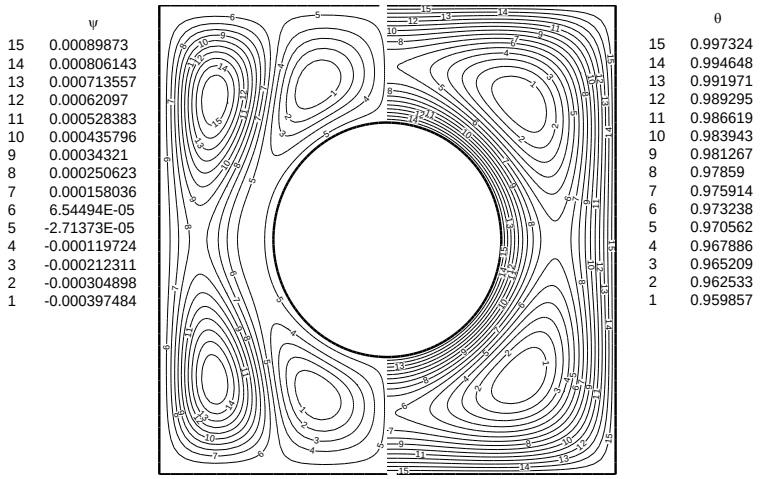

Fig.10. The Variation of the Bulk Temperature with GR.

6.3 Effect of AR:

Figs. (11-13) show the streamlines and isotherms of the fluid flow and heat transfer process. When AR is equal to 1, four cells will be generated. With variation in AR, the behavior of the streamlines will be changed. When AR decreased the two cells near the circular tube is beginning to vanish. When AR decreased less than 0.6, two cells will be occupied most the confined area between the walls of the rectangular duct and the circular tube. The intensity of these cells will be increased with decreasing in AR. While, the value of the stream function of the center of these cells will be decreased because of decreasing the confined area between the walls.

For the isotherms, it shows that when AR decreased the two cells tends to be near top and bottom the channel walls since the outer and internal boundary of this channel is closer of low values.

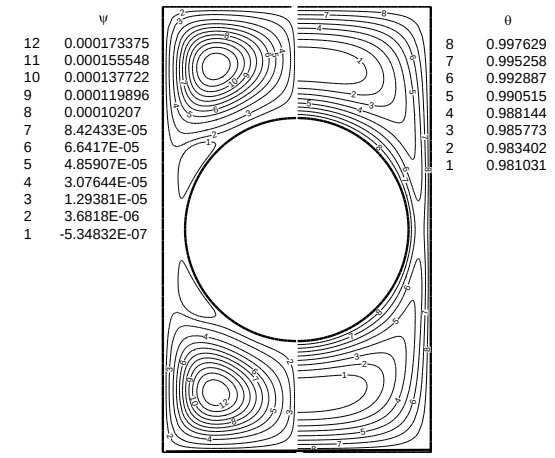

Fig.11. Streamlines and Isotherms for AR = 0.6.

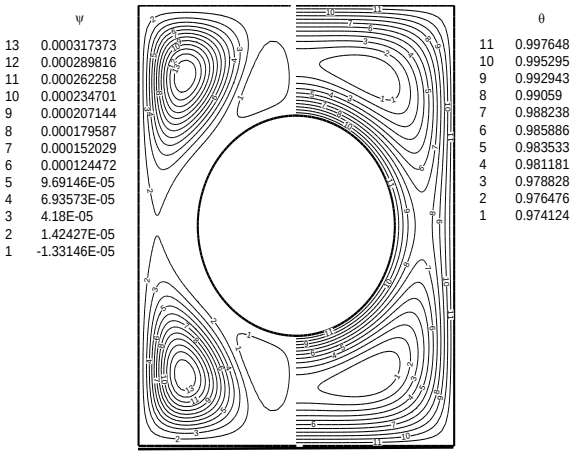

Fig.12. Streamlines and Isotherms for AR = 0.8.

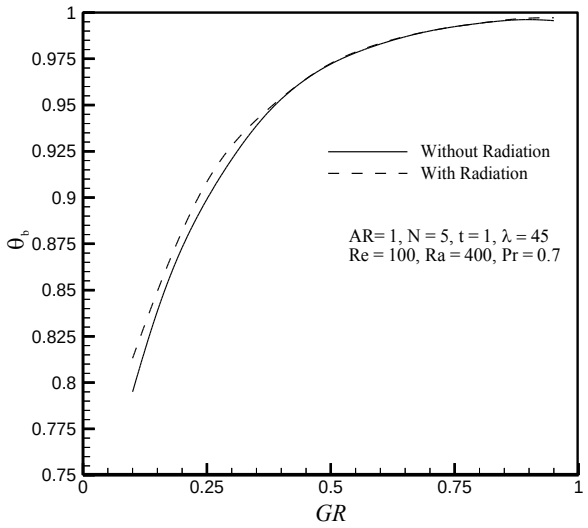

Fig.13. Streamlines and Isotherms for AR = 1.

Fig. (14) illustrates the variation in the mean value of Nu with AR. This figure shows that when AR is increased Nu will decrease because of the increasing in AR lead to increase the cross section area, and that led to increase the intensity of the air vorticity and the effect of the buoyancy force which then decrease the rate of heat transfer. The effect of radiation is noted for AR < 0.8, but with increasing in AR, the effect of radiation will be neglected.

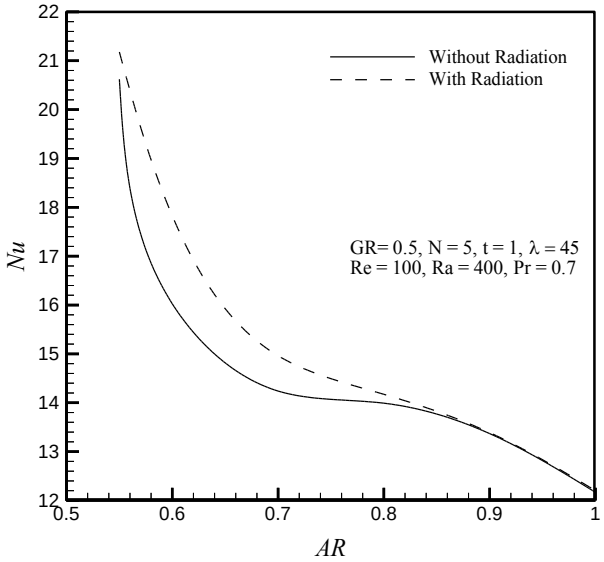

Fig.14. The Variation of Nu With AR

6.4 Radiation Effect:

The correlation equation for the plotted curves is presented to know the radiation effect on the rate of heat transfer. This equation is made by using the curve fitting method with using Data Fit program. The form of this equation is:

$$Nu = a_1 + a_2 \Omega^{a_3}$$

where a_1, a_2 and a_3 are coefficients and are tabulated in table (1).

For the bulk temperature, the effect of radiation will be written as follow:

$$\theta_b = -12.287 + 13.304 GR^{6.2\times10^{-3}}$$

(With Radiation)

$$\theta_b = -15.747 + 16.763 GR^{5.4\times10^{-3}}$$

(Without Radiation)

Table 1
The Radiation Effect

Ω	With Radiation			Without Radiation		
	a_1	a_2	a_3	a_1	a_2	a_3
GR	7.577	44.648	3.1	6.5677	39.176	2.887
AR	12.117	0.58597	- 4.55	13.0733	0.03231	- 9.0938

6.5 Effect of Radiation Properties:

Fig. (15) illustrates the effect of optical thickness t and conduction-radiation parameter N. It is shown that when t and N are increased Nu will be increased, but the increasing in t will be greater than N, this is because the optical thickness is powered to 2 into the radiation term as shown in eq.(10).

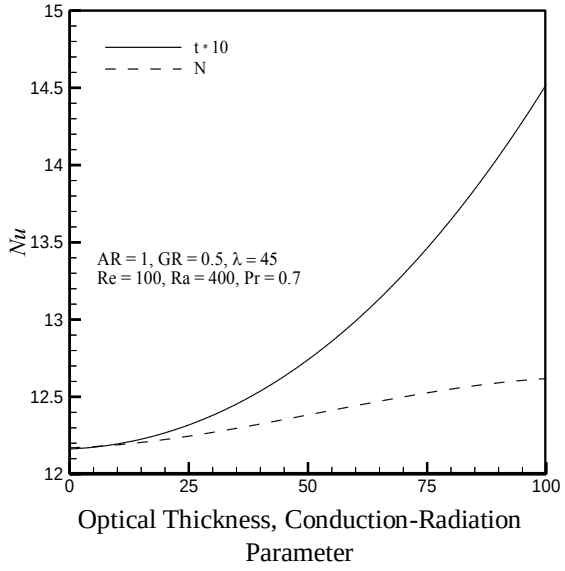

Fig.15. The Effect of Radiation Properties.

7. Conclusions:

It can be concluded from the present work that:

(1) The rate of heat transfer is increased by 87% with increasing GR from 0.1 to 0.9 and the heat transfer process is become conduction at GR = 0.9.
(2) Nu increases by 45% with decreasing in AR from 0.55 to 1.
(3) The isotherms show two cells formed for GR > 0.2 and the streamlines show two cells formed for GR < 0.4 but four cells will be generated when GR ≥ 0.4 until 0.8.
(4) The radiation effect on the heat transfer coefficient is known by making a correlation equations and this effect show that Nu will be increased.
(5) Increasing the radiation properties (t, N), the radiation effect will be also increased.

8. Nomenclature:

A	Cross-sectional area (m^2) .
AR	Aspect Ratio (L/D).
Cp	Specific heat at constant pressure (J/kg.K).
D	Major diameter (m).
d	Hydraulic diameter ($4A/ P^*$).
g	Acceleration due to gravity (m/s^2).
GR	Geometric ratio (D/L).
h	Heat transfer coefficient ($W/m^2.^oC$).
H	Height of the rectangular cross section (m).
J	Jacobean of direct transformation.
k	Thermal conductivity of the working fluid ($W/m.^oC$).
KR	Volumetric absorption coefficient (1/m).
L	Length of the rectangular cross section (m).
n	Outward normal on the wall.
N	Radiation-Conduction parameter.
Nu	Mean Nusselt number.
Nu_C	Mean Nusselt number for the circular surface.
Nu_r	Mean Nusselt number for the rectangular duct.
Nu_{LC}	Local Nusselt number.
p	The small pressure variation governing the flow distribution in

	the cross stream plane (N/m^2).
P	Average pressure over the duct cross section.
P^*	Wetted perimeter (m).
Pr	Prandtl number, $Pr = \frac{\nu}{\alpha}$.
R	Radius (m).
Ra	Rayleigh number.
Re	Reynolds number .
t	Optical thickness.
T	Dimensional fluid temperature (K).
T_i	Dimensional inlet fluid temperature (K).
T_w	Wall temperature (K).
u, v, w	Dimensional velocity in x, y and z-directions (m/s).
U, V, W	Normalized velocity in X, Y and Z-directions.
x, y, z	Dimensional Cartesian coordinates (m).
X, Y, Z	Dimensionless Cartesian coordinates.

9. Greek Symbols:

α	Coefficient of thermal expansion (m^2/s).
β	Thermal diffusivity (m^2/s).
ε	Emissivity.
ξ, η	Dimensionless Computational coordinates.
θ	Normalized fluid temperature.
θ_i	Normalized inlet fluid temperature.
θ_b	Normalized bulk temperature.
λ	Inclination to the horizontal (°).
υ	Kinematic viscosity of the fluid (m^2/s).
ρ	Fluid density (kg/m^3).
σ	Stefan Boltzmann constant (Wm^2 / k^4).
ψ	Dimensionless Stream function.
ω	Dimensionless Vorticity.

10. Supscripts:

b	Bulk
c	Circle
i	Inlet
L	Local
r	Rectangle
w	Wall
R	Radiation

11. References:

[1] Anderson A., Tannehill C. and Pletcher H. (1984), Computational Fluid Mechanics and Heat Transfer, McGraw-Hill, Washington.

[2] Bello-Ochende F. L. (1985), A Numerical Study of Natural Convection in Horizontal Elliptic Cylinders, Revista Brasileira de Ciências Mecânicas, Vol. VII, No.3,pp.185-207.

[3] Bello-Ochende F. L. and Adegun I. K. (1993), A perturbation Analysis of Combined Free and Forced Laminar Convection in Tilted Elliptic Cylinders, The 6th International Symposium on Transport Phenomena in Thermal Engineering, Seoul, Vol. III, pp.121-125.

[4] Bello-Ochende F. L. and Adegun I. K. (2002), Combined Mixed Convective and Radiative Heat Transfer in a Tilted Rotating Uniformly Heated Square Duct With a Centered Circular Cylinder International Journal of Heat and Technology, Vol. 20, No.1, pp.21-30.

[5] Dehghan A. A. and Behnia M. (1996), Combined Natural Convection–Conduction and Radiation Heat Transfer in a Discretely Heated Open Cavity, Journal of Heat Transfer, Vol. 118, pp.56-64.

[6] Dong Z. F., Ebadian M. A. and Bigzadeh E. (1993), Convective-Radiative Heat Transfer in a Square Duct with a Centered Circular Core, International Journal of Heat and Fluid Flow, Vol. 14, No. 1, pp. 68-75.

[7] Fletcher C. A. J. (1988), Computational Fluid Techniques for Fluid Dynamics 2, Springer-Verlag.

[8] Siegel R. (1985), Analysis of Buoyancy Effect on Fully Developed Laminar Heat Transfer in a Rotating Tube, Journal of Heat Transfer, Vol.107, pp. 338-344.

[9] Yang G. and Ebadian M. A. (1991), Thermal Radiation and Laminar Forced Convection in the Entrance of a Pipe With Axial Conduction and Radiation, Int. J. Heat Fluid Flow, Vol.12, No. 3 pp. 202-209.

أنتقال الحرارة بالحمل المختلط والأشعاع خلال قناة مستطيلة مائلة مع أنبوب داخلي

منال هادي الحافظ رائد كاطع صيهود
قسم الهندسة الميكانيكية/جامعة بغداد

الخلاصة

أنتقال الحرارة بالحمل الاشعاع المختلط لجريان مستقر خلال قناة مستطيلة مائلة مع أنبوب دائري داخلي متغير الموقع درست رقمياً لجريان تام التطور. تم التعامل بميكانيكية إنتقال الطاقة الحرارية بالحمل والإشعاع بشكل منفصل وفي آن واحد. المعادلات التي أستخدمت هي (الإستمرارية، الزخم ومعادلة الطاقة). تم تحويل هذه المعادلات الى معادلات بدون وحدات ثم الى صيغة دالة الإنسياب-الدوامية ثم الى صيغة الإحداثيات المطابقة للجسم. أستخدمت طريقة الفروق المحددة لإجراء جميع الحسابات باستخدام نظام مطابقة الإحداثيات لبناء شبكة النظام. تم بناء برنامج فورتران ٩٠ لحساب معامل الاحتكاك ورقم نسلت لحالة مستقرة ولنسبة شكل تتراوح بين (0.1-0.9) ولنسبة باعية (0.55-1) ولخواص جريان رقم برانتل ($Pr = 0.7$)، رقم رايلي $Ra = 400$ ، رقم رينولد $Re = 100$ ، السمك البصري $(0 \le t \le 10)$ ، معامل التوصيل- الإشعاع $(0 \le N \le 100)$ وزاوية الميل $\lambda = 45$ للمديات السابقة النتائج بينت زيادة أنتقال الطاقة الحرارية بتأثير الإشعاع وأن إنتقال الطاقة الحرارية من سطح الأسطوانة أكثر من أنتقالها من سطح المجرى المستطيل. بصورة عامة، فأن رقم نسلت سوف يزداد مع زيادة كلاً من GR ، t وN بينما يقل مع أزدياد AR. عند اضافة تأثير الاشعاع الى عملية انتقال الحرارة فأن معدل انتقال الحرارة سوف يزداد. هذا التأثير يزداد مع ازدياد قيمة GR و مع نقصان AR. أن زيادة خواص الاشعاع تؤدي الى زيادة تأثير الاشعاع و بالتالي زيادة معدل انتقال الحرارة. أستخدم برنامج تكبلوت ٧ لرسم مخططات كنتورية لدالة الانسياب و توزيع درجات الحرارة لمعرفة سلوك الهواء خلال عملية انتقال الحرارة و تغير هذا السلوك مع تغيير المعاملات المعتمدة. تم التوصل الى علاقة تصف تاثير الاشعاع على عملية انتقال الحلرارة.